Title
Optogenetic Control of Microtubule Dynamics

Authors
van Haren, Jeffrey
Adachi, Lauren S
Wittmann, Torsten

Publication Date
2020

DOI
10.1007/978-1-0716-0219-5_14

Peer reviewed

Optogenetic Control of Microtubule Dynamics

Jeffrey van Haren, Lauren Adachi, and Torsten Wittmann*

Department of Cell & Tissue Biology, University of California San Francisco, 513 Parnassus Avenue, San Francisco, CA 94143

*corresponding author

Abstract

Light can be controlled with high spatial and temporal accuracy. Therefore, optogenetics is an attractive experimental approach to modulate intracellular cytoskeleton dynamics at much faster time scales than by genetic modification. For example, in mammalian cells, microtubules (MTs) grow tens of micrometers per minute and many intracellular MT functions are mediated by a complex of +TIP proteins that dynamically associate with growing MT plus ends. EB1 is a central component of this +TIP protein network, and we recently developed a photo-inactivated π-EB1 by inserting a blue light sensitive LOV2/Zdk1 module between the EB1 MT binding domain and the +TIP adaptor domain. Blue light induced π-EB1 photodissociation results in disassembly of the +TIP complex and strongly attenuates MT growth in mammalian cells.

In this chapter, we discuss theoretical and practical aspects of how to perform high resolution live cell microscopy in combination with π-EB1 photodissociation. However, these techniques are broadly applicable to other LOV2-based and likely other blue light sensitive optogenetics. In addition to being a tool to investigate +TIP functions acutely and with subcellular resolution, because of its dramatic and rapid change in intracellular localization, π-EB1 can serve as a powerful tool to test and characterize optogenetic illumination setups. We describe protocols of how to achieve micrometer scale intracellular control of π-EB1 activity using patterned illumination, and we introduce a do-it-yourself LED cube design compatible with transmitted light microscopy in multiwell plates.

Keywords

Optogenetics, π-EB1, photodissociation, microtubules, EB1, +TIP, LOV2, LOVTRAP, Zdk1, live cell microscopy

1. Introduction

A challenge of the postgenomic era is that many intracellular processes occur at time scales that are orders of magnitude faster than the days or weeks required to deplete proteins by RNA interference or genetic deletion. Protein functions are often spatially and temporally restricted in cells, which makes mechanistic interpretation of such genetic knock-out experiments challenging. This is particularly true for cytoskeleton dynamics that operate very locally and at second to minute time scales. For example, the interphase microtubule (MT) cytoskeleton reorganizes into a bipolar mitotic spindle in typically less than 30 minutes, and individual MT bundles dynamically connect to chromosomes to ensure accurate segregation of the genetic material. Similarly, both MTs, the F-actin cytoskeleton and even much less dynamic intermediate filaments direct and respond to changes in interphase cell shape at much faster time scales than transcriptional or translational changes. Thus, experimental alteration of intracellular protein function by light is an attractive experimental approach because light exposure can be controlled with very high spatial and temporal precision.

Optogenetics originally involved expression of channelrhodopsins in neurons to elicit light-activated membrane currents and neuronal activity. However, the potential of light-modulated protein function to spatially and temporally control biochemistry in living cells is enormous, and optogenetics is no longer restricted to the neurosciences. An ever-increasing set of tools is being developed to manipulate protein interactions, localization and activity by light [1, 2].

1.1. Optogenetics with LOV2 domains

LOV domains were first identified as the light sensing units of plant light receptors of the phototropin family [3, 4]. Phototropins are blue light activated kinases, typically composed of two LOV domains (LOV1 and LOV2) in tandem followed by a serine/threonine kinase domain, and mediate plant growth towards light (phototropism), chloroplast migration and stomata opening [5]. The light absorbing unit of LOV2 domains is an obligatory flavin mononucleotide (FMN) co-factor. FMN is a riboflavin (vitamin B2) derivative, and a required co-factor in oxidoreductases in plants, animals and bacteria. Thus, FMN is ubiquitously present in most lifeforms, which simplifies LOV2-based optogenetics in mammalian systems.

Blue light exposure of the LOV2-bound FMN leads to the formation of a flavin-cysteinyl adduct between the triplet excited FMN isoalloxazine ring and a cysteine residue buried in the LOV2 core (C450 in *Avena sativa* LOV2) [6]. Adduct formation results in unwinding of the short A'α and the longer Jα helices at the LOV2 N and C termini [7–9]. Although the precise mechanism linking LOV2 photochemistry to rearrangements of protein structure is still under debate [10], the energy associated with this conformational change can be harnessed as 'optogenetic work' [11]. Several recently developed optogenetics tools have in some way made use of the switch-like conformational changes of LOV2 domains to control protein activities in a light dependent manner.

For example, LOV2 domains appended to the termini of proteins or peptides can mask a protein activity in the dark [12, 13]. Similarly, LOV2 domains inserted into protein surface loops can allosterically control protein conformation and thus activity by light [14, 15]. Finally, several LOV2 domain-based optical dimerization systems have been developed in which unfolding of the LOV2 Jα helix results in association or dissociation of small proteins that interact specifically with either the light- or dark-state LOV2 conformations [16–18].

1.2. π-EB1

To control the function and dynamics of MT-plus end-associated protein complexes with high spatial and temporal accuracy, we recently developed a novel LOV2-based optogenetic tool to reversibly inactivate protein complexes that associate with growing MT ends. In mammalian cells, the small adaptor protein EB1 (EB3 in neurons), is required to assemble complexes of so-called +TIPs at growing MT ends [19, 20]. EB1 is a dimer with an N-terminal domain that recognizes the guanosine nucleotide state of growing MT ends, and a C-terminal domain that recruits +TIP proteins. We designed a light-sensitive variant of EB1 by connecting these two EB1 functional domains with the light-sensitive LOVTRAP module (Fig. 1) [16, 21]. This results in rapid and reversible blue-light induced dissociation of the C-terminal π-EB1 part and associated +TIPs from growing MT ends (Fig. 2b). In addition, we found that in the cell types we tested so far, π-EB1 photodissociation results in substantial inhibition of MT growth, and we propose that π-EB1 can thus be utilized to dissect the intracellular functions of +TIP complexes at high spatial and temporal accuracy. However, it is important to note that observing functional effects of π-EB1 photodissociation requires replacing endogenous EB1/3 activity with π-EB1. We recently published protocols how this can be done using RNA interference or CRISPR/Cas9 genome editing [22], and we will not describe this here. Instead, we are focusing on the technical aspects of how we perform optogenetics experiments on a microscope using π-EB1 as an example. We believe that these concepts and protocols can be adapted to other LOV2-based and likely other blue light-controlled optogenetic systems.

1.3. General considerations using LOV2 domains

In addition to LOV2 domains, many other plant and bacterial light sensors have been developed into optogenetic tools. While no single system is perfect, we find that the small size and high solubility in combination with fast switching kinetics and the ubiquitous FMN co-factor makes LOV2 domains ideal to achieve subcellular spatial control in mammalian cells. Next, we discuss some of the characteristics of LOV2 domains that need to be considered when planning an experiment with π-EB1 or other LOV2-based systems.

1.3.1. Spectral response

The spectral response of LOV2 domains is determined by the FMN spectrum, which also makes it unlikely that red-shifted LOV domain variants are possible. Although FMN peak absorption is around 440-470 nm, the excitation spectrum reaches into the UV and above 500 nm (Fig. 2a). In live fluorescence imaging experiments,

this limits the fluorescent proteins (FPs) that can be used in combination with LOV2 optogenetics to red and far red FPs with excitation wavelengths above 550 nm, or red and far red SNAP or HALO tag compatible fluorescent dyes [23]. Blue, cyan and green fluorescent proteins are essentially incompatible as their excitation wavelengths very efficiently photoactivate LOV2. In our hands, even 515 nm yellow FP excitation resulted in π-EB1 photodissociation albeit less efficiently and should probably not be used in combination with LOV2 optogenetics (Fig. 2b). To be safe, we use a red filter in the transmitted lightpath for extended transmitted light imaging although at least wild-type LOV2 does not seem to be activated efficiently by the blue light component in typically used transmitted light intensities. However, the broad LOV2 spectral response has the advantage that at least temporal photoactivation control can be easily implemented on any microscope that has a GFP excitation channel.

1.3.2. Kinetics

The photochemistry underlying LOV2 photoactivation is very fast with formation of the flavin-cysteinyl adduct in the microsecond range [8, 24, 25]. While recent work shows that initial unfolding of the Jα helix happens concurrently with adduct formation, full unfolding occurs in the millisecond range in isolated LOV2 domains [8, 26]. However, subsequent conformational changes and association/dissociation of effector proteins are likely substantially slower, as they depend on the binding kinetics and diffusion rates of the molecules involved. In the case of π-EB1, we measured a blue-light-induced photodissociation half-life of <200 ms. However, reassociation of π-EB1 after blue light exposure is much slower as this depends on both the dark state recovery of LOV2 (*see* **Note 1**) as well as the two π-EB1 halves finding and binding to each other. In our original π-EB1 design, we used a LOV2 domain with a Jα helix-stabilizing LAAA N terminus [18] for which we measured a half-life of π-EB1 dark reassociation of around 10 seconds. It is important to be aware of these kinetics as they affect both spatial and temporal resolution of subcellular optogenetics experiments. In addition, in most cases we use pulsed blue light illumination to control light exposure dose, minimize phototoxicity, and avoid crosstalk with imaging channels. With this original π-EB1 design, a pulse frequency of 1 Hz is enough to keep average π-EB1 activity below 3%. However, one needs to be aware that the relative amount of dissociated π-EB1 is not constant, and gradually decreases until the next blue light exposure depending on pulse frequency and π-EB1 reassociation rate (Fig. 3c). Using a LOV2 variant with a faster dark state recovery rate, we were able to reduce the dark recovery half-life by a factor of two. However, one should bear in mind that keeping a fast LOV2 domain activated will require more frequent light exposure. In addition, dark recovery of other LOV2-based optogenetics systems may be much faster especially if they only involve single molecule conformational changes, and on and off kinetics should always be characterized to determine the optimal photoactivation illumination sequences.

1.3.3. Temperature

Although the photochemistry underlying LOV2 photoactivation is largely temperature insensitive within the biological range, the thermal decay of the flavin-cysteinyl adduct in the dark is not and occurs substantially slower at lower temperature (Fig. 3a) [6, 27]. However, somewhat surprisingly, we also found that while π-EB1 photo-dissociation occurred very rapidly in mammalian cells at 37 °C, it was much slower and incomplete at lower temperatures (Fig. 3b). We do not fully understand why this is the case, but it may be related to a decreased LOV2/Zdk1 off-rate at decreased temperature. This is further supported by our finding that photodissociation of π-EB1 with a wild-type LOV2 domain with LATT N terminus that was originally used to develop LOVTRAP and likely has a higher affinity for Zdk1 is even less efficient at room temperature. It is possible that this temperature sensitivity is specific to the LOVTRAP system in which thermal energy facilitates LOV2/Zdk1 photodissociation. From a practical point of view, this is important when these systems are adapted to non-mammalian experimental models with lower temperature optimum such as fruit flies, nematodes or zebrafish. To verify that an optogenetic system works as anticipated in a given experimental system, it is therefore highly recommended to have a direct microscopy-based assay in place – such as blue light induced dissociation of the π-EB1 C-terminal half from MT ends (Fig. 2b).

1.3.4. Phototoxicity

Phototoxicity is always a concern in live imaging experiments, especially with higher energy blue light [28]. In general, we find that the amount of light energy required for π-EB1 photodissociation is substantially lower than what is typically used for fluorescence imaging. For example, a single 100 ms exposure at 0.1-1 W mm^{-2} irradiance, which is a typical light intensity range in both epifluorescence or spinning disk confocal microscopy [29], amounts to a radiant exposure of 10-100 mJ mm^{-2} for each image taken. In contrast, we find that π-EB1 can be efficiently maintained in the dissociated state by short blue light pulses with energies below 0.2 mJ mm^{-2} [21]. However, to maintain π-EB1 photo-dissociation these blue light pulses must be administered at a frequency of 1 Hz or higher (Fig. 3c). Thus, in short term experiments or experiments utilizing spatially patterned blue light, radiant exposure is quite low and likely negligible, but in longer term experiments the accumulated radiant energy becomes substantial (i.e. 3600 pulses per hour equals 720 mJ mm^{-2}). Slower, more light-sensitive LOV2 variants requiring less frequent blue light exposure may therefore be better suited for long-term experiments [30, 31]. It should also be noted that different cell types may have very different sensitivities to blue light. In addition, one should be aware that common cell culture media ingredients such as riboflavin are strong blue light photosensitizers. Strikingly, riboflavin-mediated generation of reactive oxygen species and hydrogen peroxide in blue light is further exacerbated in the presence of HEPES [32–34], which is frequently used to buffer cell culture media without 5% CO_2 during microscopy experiments. Blue light mediated reactive oxygen generation may be particularly problematic in experiments using bulk blue light illumination of entire

dishes or wells that would generate significant amounts of phototoxic compounds throughout the culture medium volume. For such experiments it is likely indicated to use special media formulations that reduce the concentration of photosensitive compounds [35]. In any case, control experiments with cells not expressing the light-sensitive construct at identical blue light exposure conditions must always be included.

2. Materials

It is difficult to present a comprehensive list of materials for live cell microscopy experiments and the following should be seen only as guidelines that will need to be adapted for specific experimental questions.

2.1. Plasmids

1. π-EB1 plasmids:

pEB1N-LZ-LOV2(wt)	(Addgene #107614)	LAAA N terminus
pEB1N-LZ-LOV2(fast)	(Addgene #107690)	
pmCherry-Zdk1-EB1C	(Addgene #107695)	
pEGFP-Zdk1-EB1C	(Addgene #107696)	

2. EB1/3 shRNA and CRISPR plasmids:

pLKO.1 EB1 shRNA #3	(Addgene #37927)
pSpCas9_BB_2A_GFP_MAPRE1-gRNAs	(Addgene #107726, 107727, and 107728)
pSpCas9_BB_2A_GFP_MAPRE3-gRNAs	(Addgene #107729, 107730, and 107731)

3. Original LOVTRAP plasmids:

pTriEX-NTOM20-LOV2	(Addgene #81009)	LATT N-terminus
pTriEX-mCherry-Zdk1	(Addgene #81057)	

2.2. Cell culture

1. H1299 lung cancer cells (ATCC CRL-5803); or other mammalian cell line.
2. RPMI-1640 medium with 10% FBS, 1x Penicillin/Streptomycin, 1x non-essential amino acids (NEAA); or medium as appropriate for different cell lines.
3. Transfection reagent (Fugene-6 or as required for other cell lines).
4. Reduced serum transfection media (e.g. Opti-MEM).

2.3. Microscopy

1. Inverted spinning disk confocal microscope. For a more detailed description of our system with a Borealis-modified Yokogawa CSU-X1, Photometrics cMyo CCD camera, ASI MS-2000 motorized stage, and an environmental enclosure on a Nikon Ti-E stand, see [36].
2. Digital micromirror device (DMD) pattern illuminator (e.g. Mightex Polygon400) with a blue 470 nm light source.

3. Imaging software that can control microscope and DMD device.
4. Light power meter (e.g. X-Cite XR2100).
5. Microscopy medium with reduced auto-fluorescence (e.g. FluoroBrite DMEM) supplemented with 10-20 mM HEPES buffer if CO_2 control is not available on the microscope.
6. Glass bottom dishes (e.g. MatTek P35G-1.5-20-C).
7. Glass bottom 12-well plates with black plastic frame to prevent cross-illumination between wells (e.g. Cellvis P12-1.5H-N).
8. Dow Corning high vacuum grease in a 10-ml plastic syringe.
9. Yellow highlighter marker (e.g. Stabilo Boss) to visualize DMD patterns by fluorescence.
10. Black marker (e.g. Sharpie) to help with focusing on coverglass surface.

2.4. Miscellaneous materials for LED cube and triggering

1. Arduino UNO microcontroller with external 9V power supply.
2. TTL output from imaging computer (we use a National Instruments USB-6501 digital I/O board that is also used to control lasers and other shutters on our system).
3. Prototyping Breadboard and jumper wires.
4. 3 mm 60° viewing angle 470 nm LEDs (> 1cd brightness), for example Visual Communications Company VAOL-3LSBY4.
5. 24 V DC (500 mA - 1A) power supply to power the LED circuits.
6. Resistors (100 – 1000 Ω, 1/4 W)
7. Low power general purpose NPN switching transistor (e.g. 2N2222A)
8. 3D printer (often accessible in Maker lab spaces)
9. 15 mm round coverglasses (e.g. Warner Instruments)

3. Methods

Since every fluorescence microscope will have a blue light excitation channel for imaging of GFP or similar fluorophores, the most basic implementation of LOV2 photoactivation with temporal control can be accomplished relatively easily on most microscopes. Spatial targeting of subcellular regions of interest however requires additional equipment to project blue light patterns onto the image plane of the microscope. Finally, controlling larger regions beyond the objective field-of-view also requires a different blue light illumination setup to allow simultaneous blue light exposure of larger areas or multiple wells while being compatible with specific imaging requirements. Here we focus on the technical aspects how we perform these three different types of optogenetics experiments.

3.1. Temporal π-EB1 photoinactivation using microscope illumination

Any inverted fluorescence microscope will work for this. We use spinning disk confocal microscopy to clearly visualize MT plus end associated π-EB1, but it should be possible to see EB1 plus end tracking with a conventional epifluorescence microscope equipped with high NA 60x or 100x oil immersion objectives. To test π-EB1 photodissociation cells can simply be transfected with plasmids encoding the N- and C-terminal π-EB1 halves, which we describe here. However, experiments assessing the function of EB1 +TIP complexes requires removing endogenous EB1 (and possibly EB3). H1299 lung cancer cells in which endogenous EB1 has been depleted by either RNA interference or genetic knockout and replaced with π-EB1 are available on request. For procedures to establish these π-EB1 cell lines see [22]. All required plasmids are available on Addgene (*see* **Materials**).

1. Seed cells on a 3.5 cm glass bottom dish at ~10% confluency, place in 37 °C, 5% CO_2 incubator overnight.
2. The next day co-transfect with plasmids encoding π-EB1 halves. Prepare transfection mix in a 1.5-ml Eppendorf tube (one per dish): Add 3 µl Fugene 6 to 100 µl Opti-MEM. Mix well. Add 1.5 µg EB1N-LOV2 and 0.5 µg mCherry-Zdk1-EB1C (*see* **Note 2**). Mix well. Incubate for 15 min at room temperature. Add transfection mix dropwise to cell culture dish and return to incubator. Note that different types of cells will require different types of transfection procedures.
3. The next day, prepare the dish for microscopy by replacing the medium with low fluorescence FluoroBrite DMEM. To avoid medium evaporation, we also often seal the lid of the dish onto the bottom by squeezing a bead of vacuum grease around the inside edge of the lid before closing.
4. Place dish in environmental chamber on the microscope stage and let equilibrate for 10 min.
5. Using the optical configuration for imaging red fluorescent proteins (λ_{Ex} > 550 nm), look for cells that show the typical EB1 comet pattern in cells (*see* Fig. 2b). MT plus end localization of the mCherry-tagged C-terminal half indicates that the untagged N-terminal half is expressed at sufficient levels (*see* **Note 3**).
6. Set up a time-lapse experiment with two phases with 1 frame per second acquisition rate using filter sets for multi-band GFP and RFP excitation (i.e. λ_{Ex} = 488 and 561 nm) and RFP emission (λ_{Em} > 580 nm). Each phase should be 20-30 s long with 200-400 ms exposure times:
   Phase 1: only 561 nm excitation is on for imaging mCherry-Zdk1-EB1C; 488 nm light source is off.
   Phase 2: both 561 nm and 488 nm light sources are on for LOV2 photoactivation (*see* **Note 4**).
7. Run imaging experiment.

The expected outcome is that mCherry-Zdk1-EB1C tracks growing MT ends in phase 1, but rapidly dissociates from MT ends in phase 2 when the 488 nm illumination source has been turned on (*see* Fig. 2b). The 488 nm light source should be adjusted to the minimal intensity that shows complete mCherry-Zdk1-EB1C dissociation in

2-3 images. In our Borealis-modified spinning disk setup that amounts to 10% power of the 100 mW 488 nm laser (~2 mW mm^{-2} in the image plane) with <200 ms exposure times [36].

3.2. Spatial π-EB1 photoinactivation using a digital micromirror device (DMD)

Spatial control requires projecting light patterns of interest onto the specimen plane. While this can be accomplished using a point scanning system, we find that especially for the low light intensities required for LOV2 photoactivation, a digital micromirror device (DMD) based illuminator is the most versatile and practical solution. Most commonly a DMD pattern illuminator is coupled into the microscope through a secondary epifluorescence port. In Nikon microscopes this is realized through two filter turrets stacked on top of each other. However, our system is a little unconventional in that we use a secondary camera port in the eyepiece lightpath to connect an older model Polygon400 pattern illuminator with a built-in 1 W 470 nm LED (Fig. 4b). Using an 80/20 beamsplitter in the emission lightpath, this has the advantage that the blue light pattern can be imaged directly with the spinning disk camera (Fig. 4c), which makes it very easy to focus the DMD pattern on the image plane, but it does require manual switching between eyepieces and DMD port before starting an experiment. Another disadvantage is that only 20% of the blue light pattern intensity reaches the specimen, but as outlined below this is still more than enough for LOV2 photoactivation.

3.2.1. Visualizing and focusing the DMD blue light pattern

In our setup, the blue light pattern can be directly imaged through the spinning disk microscope. However, if the DMD device is coupled through the epifluorescence excitation lightpath, it will likely be very difficult to directly image the blue light pattern reflection because the UV-selective dichroic mirror, which directs the excitation light from the DMD device to the specimen, will also prevent most light reflected back from the coverglass from reaching the camera. In this case fluorescence from a yellow/green highlighter marker can be used to visualize the pattern.

1. Mark a glass bottom dish with fluorescent highlighter. Omit if directly imaging the blue light reflection. Place the dish on the microscope stage.
2. Set up imaging in the GFP channel but turn off the 488 nm excitation laser. If directly visualizing the blue light reflection, also remove the GFP emission filter from the lightpath. Start live imaging.
3. Focus on the top coverglass surface using the camera and transmitted light. A mark with a black Sharpie marker helps with focusing. It is not terribly important if this is the top or bottom surface reflection. It is only important that the camera chip and the DMD chip end up parfocal.
4. Turn off transmitted light. Turn on blue light pattern (*see* **Note 5**).
5. Refocus on the blue light pattern as much as possible.

6. Carefully slide the DMD device in the focus tube to obtain the sharpest possible image. Also turn sideways to align with the camera angle as much as possible. Best results likely require a few iterations of Steps 5 and 6. Once satisfied, tighten set screws on the DMD focus tube.

3.2.2. Measuring irradiance at the specimen plane

To minimize phototoxicity and achieve maximal spatial control, it is important to determine the optimal pulse frequency and light exposure, and thus to characterize the illumination setup as accurately as possible. The light power at the specimen plane can be measured with a light meter. However, this is only informative if we also know the area of the exposed surface. The amount of light power received per surface area is defined as irradiance (in W per unit area).

1. Using the procedure described above, take an image of the reflection (or fluorescence) of a rectangular blue light pattern.
2. Calculate the area of the blue light pattern in μm^{-2}. This requires knowledge of the calibrated pixel size. If there is no intermediate magnification in the light path, this should be very close to the pixel size of the camera divided by the objective magnification.
3. Remove coverglass or dish. If an oil immersion lens was used, carefully wipe the oil off the objective. Do not put immersion oil on the light sensor!
4. Place the sensor of the microscope light meter on the microscope stage with the sensor window facing toward the objective. Set the light meter to the correct wavelength (i.e. 470 nm). While the sensor of the light meter should not be too far from the focal plane, it does not have to be perfectly in focus. The photon flux in and out of focus is the same, only spread over a different area.
5. Turn on the same photoactivation pattern in continuous mode, not pulsed, to measure light power.
6. Calculate irradiance by dividing the power reading by the area of the blue light pattern. Example: The light meter reads 5 mW. The pattern is a square with 500 µm sides. Thus, the irradiance is 5 mW divided by 0.25 mm^2, or 20 mW mm^{-2}. Beware of the squares of metric prefixes.

While we can measure the irradiance of different photoactivation setups, it is important to remember that irradiance characterizes the brightness at the specimen plane but does not by itself inform how much light energy is received by the specimen as that also depends on the amount of time of irradiation. The amount of light energy received is defined as radiant exposure (J per unit area), which is the irradiance multiplied by the exposure time.

We typically use the DMD LED at the lowest power setting. With a 60x 1.49 NA oil immersion lens, this gives us an irradiance at the specimen plane of just below 20 mW mm^{-2}. Thus, a single 10 ms blue light pulse delivers a

radiant exposure of almost 0.2 mJ mm^{-2}, and one hundred 10 ms pulses will deliver a cumulative 20 mJ mm^{-2} (*see* **Note 6**). Both irradiance and radiant exposure should be reported in optogenetics experiments (*see* **Note 7**). Statements in experimental procedures of percent laser power used or even light power coming out of the objective are essentially meaningless, contain no information about the amount of light energy a sample was exposed to, and should be avoided.

3.2.3. Blue light triggering

Most light sources including LEDs have only a limited and non-linear range of intensity control. Thus, the best way to control the amount of blue light exposure is by modulating exposure time at a fixed intensity. In addition, to prevent interference of the blue light pattern with image acquisition (we observe some scattered blue light in the RFP channel, and 470 nm light excites RFP fluorescence to some extent), it is best to time patterned blue light exposures such that they occur in between image acquisitions (Fig. 4a). Depending on the experiment, different hardware solutions may have to be implemented to trigger blue light pattern pulse sequences:

Fast time-lapse: For short experiments with relatively high acquisition frequency (e.g. MT dynamics at 2 frames per second image acquisition rate), the blue light pattern can be directly triggered by a high-to-low edge TTL output when the camera has finished image exposure. Most scientific cameras provide such a TTL signal, but the name varies by manufacturer (Photometrics calls it 'Expose out'). In this case, the blue light pulse frequency is determined by the image acquisition frequency and needs to be sufficiently high to maintain π-EB1 photodissociation (i.e. >1 Hz for π-EB1; *see* Fig. 3c). It is also important to make sure that there is enough time in between images for the blue light pulse (i.e. a 300 ms image exposure at 2 frames per second leaves 200 ms for the blue light pulse). In addition, a trigger delay can be set to temporally shift the blue light pulse away from the image acquisition window.

Slow time-lapse: For longer experiments with lower acquisition frequency (e.g. cell migration at 1 frame per minute or less), it is necessary to utilize an external pulse generator at at least 1 Hz if π-EB1 photodissociation is to be maintained. Such a pulse generator can be quite easily implemented using an Arduino microcontroller similar to what we describe below (*see* Fig. 5c; the output pin 5 of the Arduino board would then directly connect to the trigger-in of the Polygon400). However, because the Polygon400 is unresponsive to external triggers once a blue light pulse has started, the timing of blue light pulses in relation to the imaging frame rate must be careful planned to avoid overlap with the next image acquisition. In addition, the pulse generator should be synchronized after each image exposure, otherwise small timing inaccuracies will eventually result in overlap.

3.3. LED cube design for multiwell plate photoactivation

Because blue light exposure through the objective only allows for photoactivation of one field-of-view at a time, especially long-term experiments observing cell behavior over several hours become very low throughput. Photoactivation of larger areas or multiple wells (to allow for control and experimental conditions in parallel) therefore requires an external light source. To further permit transmitted light imaging in combination with π-EB1 photodissociation, we designed a 3D printed LED cube that fits over two wells of a 12-well glass bottom plate (Fig. 5a,b). This design in which an observation window is surrounded by six 3 mm LEDs allows simultaneous and more or less evenly distributed blue light exposure and transmitted light imaging of two complete wells. The observation window can further be covered with a 15 mm coverglass to minimize media evaporation, and the LED-cube fits inside an Okolab stage top incubator. Pulse frequency and duration are controlled by an Arduino UNO microcontroller that also takes a TTL input from a shutter or the imaging software to switch photoactivation on and off, and a TTL input from the camera to turn off the blue LEDs when an image is taken (Fig. 5c; *see* **Notes 8** and **9** for a more detailed explanation of the control circuit and corresponding Arduino code, respectively).

Because the blue light is spread over a much larger area the irradiance in this LED cube setup is substantially lower than what is achieved with the DMD device. Even though we are using some of the brightest available LEDs with a wide viewing angle, the power measured with a light sensor just below the glass bottom is <15 mW. The diameter of the EXFO light sensor is 1 cm (i.e. the area is 78.5 mm^2), which gives an irradiance of a little less than 0.2 mW mm^{-2}. This is approximately 100 times less than what we typically use with the DMD. Thus, to achieve a similar radiant exposure per blue light pulse, pulse length with this LED cube has to be much longer. Empirically, we find that 400 ms blue light pulses are enough to achieve sustained π-EB1 photodissociation.

Finally, it is important to note that even these low power LEDs dissipate a significant amount of heat resulting in an increase in sample temperature. Because we directly measure sample temperature with a thermocouple submersed in one of the blue light exposed wells (adjacent wells will not reflect temperature in the illuminated wells), feedback to the heating system eventually returns temperature to the set point. We were also able to largely compensate for this transient temperature increase by temporarily turning off the heating of the stage top incubator at the same time as the blue light exposure is turned on (Fig. 5d).

4. Notes

1. Many LOV2 mutations have been identified that affect the dark state recovery rate, with half-lives from 2 seconds to over 30 minutes [30, 31, 37]. One must be aware though that most of these LOV2 mutants have not been characterized well in the context of optogenetic switches and that slower LOV2 variants will be much more sensitive to ambient light and extended transmitted light imaging. In this case, a red filter is strongly recommended.
2. Transient transfection with untagged EB1N-LOV2 and mCherry-Zdk1-EB1C is a simple and useful way to characterize the photoactivation setup. However, for making cell lines in which endogenous EB1 is replaced by π-EB1 to optically control MT dynamics, we have used EGFP-Zdk1-EB1C in combination with an untagged version of EB1N-LOV2 instead. While this does not allow observation of EGFP-Zdk1-EB1C MT plus end tracking, it is possible to acquire single images in the GFP channel to evaluate MT end localization and ensure that π-EB1 photodissociation works as expected. A GFP tag also greatly facilitates FACS sorting and clonal selection. Most importantly, labeling π-EB1 with GFP leaves the mCherry channel available for other markers of interest. In π-EB1 without endogenous EB1 (and EB3), other mCherry-tagged +TIPs should disappear from growing MT ends as a consequence of π-EB1 photodissociation. In addition, for analyzing MT organization and growth dynamics, we transiently transfect mCherry-tubulin, or an mCherry-tagged version of the π-EB1 N-terminal half, which remains bound to MT ends in the presence of blue light.
3. No MT end localization of mCherry-Zdk1-EB1C after a few minutes of no blue light exposure indicates that EB1N-LOV2 is not expressed. mCherry-Zdk1-EB1C localization along MTs indicates too high expression levels.
4. In Nikon NIS Elements, the software we use to control our microscopes, this can be done by defining two consecutive time phases in the ND acquisition dialog. In the advanced settings, a macro is executed that changes 488 nm laser power from 0% to 10% between the two time phases.
5. We are using a first-generation Polygon400 that can only be controlled by the (now obsolete) Mightex PolyLite software. This requires that a transparent DMD ROI window is aligned and overlaid with the camera window in the imaging software to draw and target patterns. There are surely much more elegant ways to do this, but this is the cheapest and requires no software integration. To turn on the pattern continuously in PolyLite, we use autotrigger mode and set trigger period and pulse duration to the same value.
6. When measuring irradiance on the microscope, one must keep in mind that photon flux density scales with the square of objective magnification. Because of the difference in area, with the same light source,

the irradiance with a 10x objective is 36-fold smaller than with a 60x objective. In other words, a 10 ms blue light pulse at 60x will deliver the same amount of energy per unit area as a 360 ms pulse at 10x.

7. Confusingly, for pulsed light exposure irradiance is sometimes multiplied by the pulse duty cycle and expressed as 'average irradiance', i.e. a 1 Hz sequence of 10 ms pulses has a 1% duty cycle and at 100 mW mm^{-2} would have a 1 mW mm^{-2} 'average irradiance'. However, this becomes very confusing when one wants to figure out the light energy received by a specimen. It seems more meaningful for both regular microscopy experiments and optogenetics to report the radiant exposure received by the sample.
8. Control of a low power LED array is implemented as a low side transistor switch using low-cost components and can be easily implemented on a prototyping breadboard. In this example, the LED pulse sequence is controlled by an Arduino microcontroller, but any other TTL pulse generator should work equally well. The value of the current limiting resistor in the LED series depends on the power ratings of the specific LEDs. We used six 3 mm through hole 470 nm LEDs from Visual Communications (VCC) with 1200 mcd luminous intensity, forward current I_f = 20 mA, forward voltage V_f = 3.5 V. The value of the current limiting resistor is calculated as $R = (V_{supply} – n_{LEDs} \cdot V_f) / I_f = (24\ V – 6 \cdot 3.5\ V) / 0.02\ A = 150\ \Omega$. We use 1/4 W resistors to be on the safe side. These LEDs have a 60° viewing angle to cover the bottom of the dish as evenly as possible. The 2N2222A NPN transistor is rated up to 40 V and 600 mA, so it should be able to handle many of these LED circuits in parallel.
9. Arduino code to control LEDs using the circuit shown in Fig. 5c is listed below. Shutter is a software controlled TTL output. In this case, the Arduino board does not have to be connected to the imaging computer and can stand alone. However, if a TTL output is not available this could also be implemented directly as a serial command to the Arduino board. Multiple different pulse sequences can be programmed onto different output pins in parallel. Time measurements in milliseconds are not entirely precise on Arduino, which counts time in 1.024 ms increments. To avoid drift over longer time periods, the LED pulse cycle is reset after each camera exposure.

```
class Blues
{
  int ledPin;                // the number of the LED output pin
  long OnTime;               // Time LED is turned on in milliseconds
  long OffTime;              // Time LED is turned off in milliseconds
  int trigState;
  int camCurr;
  int camLast;
  int shuttState;
  unsigned long previous;    // last time LED was updated

  public:
```

```
  Blues(int pin, long on, long off)
  {
  ledPin = pin;
  pinMode(ledPin, OUTPUT);

  OnTime = on;               // transfer and initialize variables
  OffTime = off;
  trigState = LOW;
  camCurr = LOW;
  camLast = LOW;
  shuttState = LOW;
  previous = 0;
  }

void Update()
  {
    unsigned long current = millis();
    if ((trigState == HIGH) && (current - previous >= OnTime))
    {
      trigState = LOW;             // time to turn LED off
      previous = current;          // remember the time
    }
    if ((trigState == LOW) && (current - previous >= OffTime))
    {
      trigState = HIGH;            // time to turn LED on
      previous = current;          // remember the time
    }

    shuttState = digitalRead(8);   // read external shutter state from pin 8
    camCurr = digitalRead(12);     // read camera exposure state from pin 12

    if ((camCurr == LOW) && (shuttState == HIGH) && (trigState == HIGH))
    {
    digitalWrite(ledPin, HIGH);
    }        // turn on LED only if shutter is on and camera is not exposing
    {
    digitalWrite(ledPin, LOW);
    }

if ((camLast == HIGH) && (camCurr == LOW))
    {
    previous = 0;
    }                            // reset time after camera exposure

camLast = camCurr;               // remember previous camera state
  }
};

Blues led5(5, 400, 600);     // define output channel pin 5 at 1 Hz 400 ms on

// define additional output channels
// Blues ledX(pin number, time on in ms, time off in ms)

void setup()
{
  pinMode(8, INPUT);             // set shutter input pin
  pinMode(12, INPUT);            // set camera input pin
```

```
}

void loop()
{
  led5.Update();                  // update LED state

// update additional output channels
// ledX.Update();
}
```

Acknowledgements

This work was supported by NIH grants R01 GM094819, R01 NS107480 and R21 CA224194 to T.W. We would also like to thank Dylan Romero and Jenny Tai from The Makers Lab at UCSF for valuable advice and assistance with 3D printing.

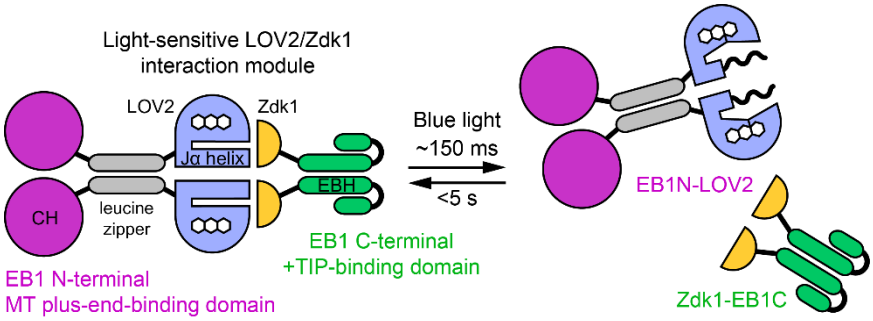

Fig. 1 Schematic of π-EB1, a split version of the MT plus end tracking protein EB1, in which the N-terminal MT-plus end binding (CH) domain is fused to the *A. sativa* phototropin 1 LOV2 domain. This N-terminal part also includes a short leucine zipper to maintain dimerization in the photodissociated state. The C-terminal +TIP adapter (EBH) domain is fused to Zdk1 (and a fluorescent protein). In the absence of blue light, Zdk1 and LOV2 domains bind with high affinity, thereby reconstituting a functional EB1 module that associates with growing MT plus ends, and is able to recruit other +TIP proteins to the MT end. In the presence of blue light, LOV2 and Zdk1 dissociate thereby splitting the π-EB1 complex rapidly and reversibly due to the spontaneous dark state recovery of the LOV2 domain. Adapted from [21].

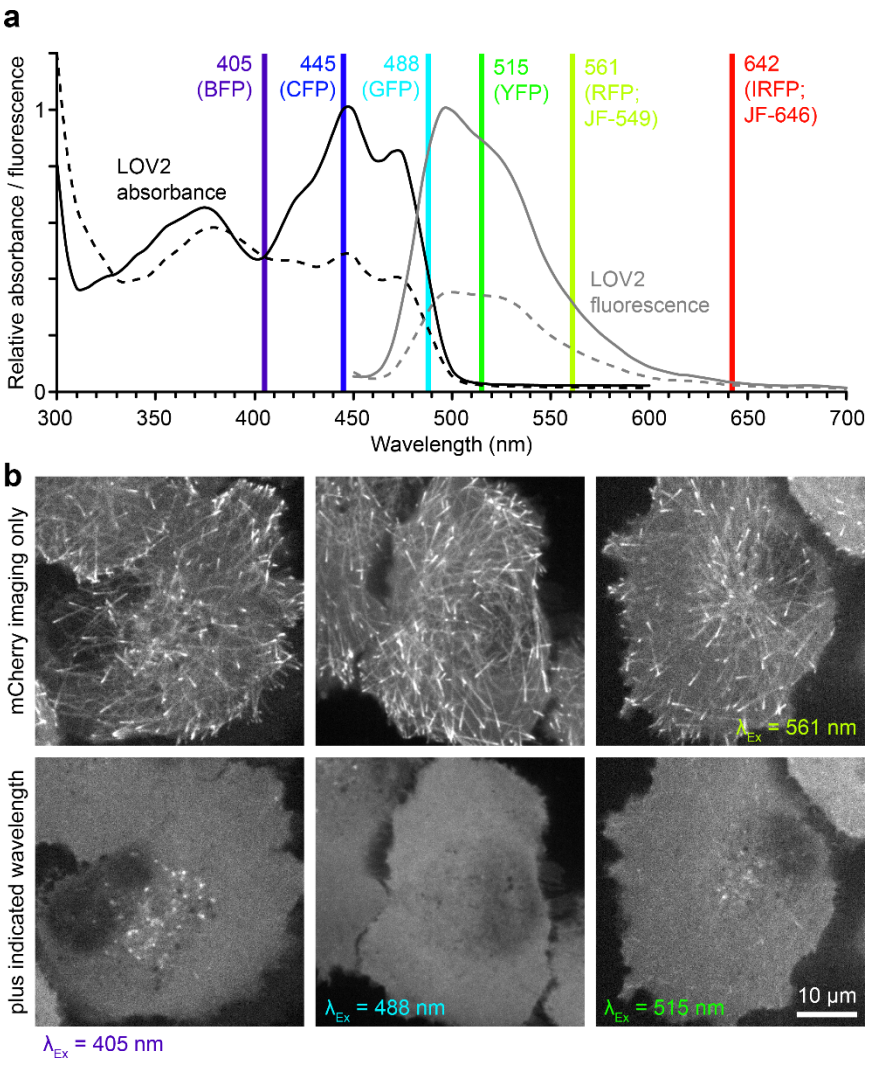

Fig. 2 LOV2 domain spectral response and compatibility with fluorescence microscopy. (**a**) Absorbance (black lines) and fluorescence spectra (grey lines; λ_{Ex} = 405nm) of purified GST tagged *A. sativa* phototropin 1 LOV2 domain, before (solid lines) and after (dashed lines) 10s of blue light illumination with a 36W 460nm LED lamp. The flavin-cysteinyl adduct no longer absorbs blue light and thus quenches LOV2 fluorescence. Laser lines commonly used in fluorescence microscopy are indicated. (**b**) π-EB1 photodissociation by different wavelengths in cells expressing untagged EB1N-LOV2 and mCherry-Zdk1-EB1C. mCherry-Zdk1-EB1C was imaged before (top) and after (bottom) switching on the other wavelength. Note that even 515 nm light at the tail end of the LOV2 absorbance spectrum (only ~3% of the peak absorbance) still results in π-EB1 photodissociation although much less efficiently than shorter wavelengths. This makes YFP a risky choice for live cell imaging in combination with LOV2 optogenetics, especially at higher acquisition frame rates.

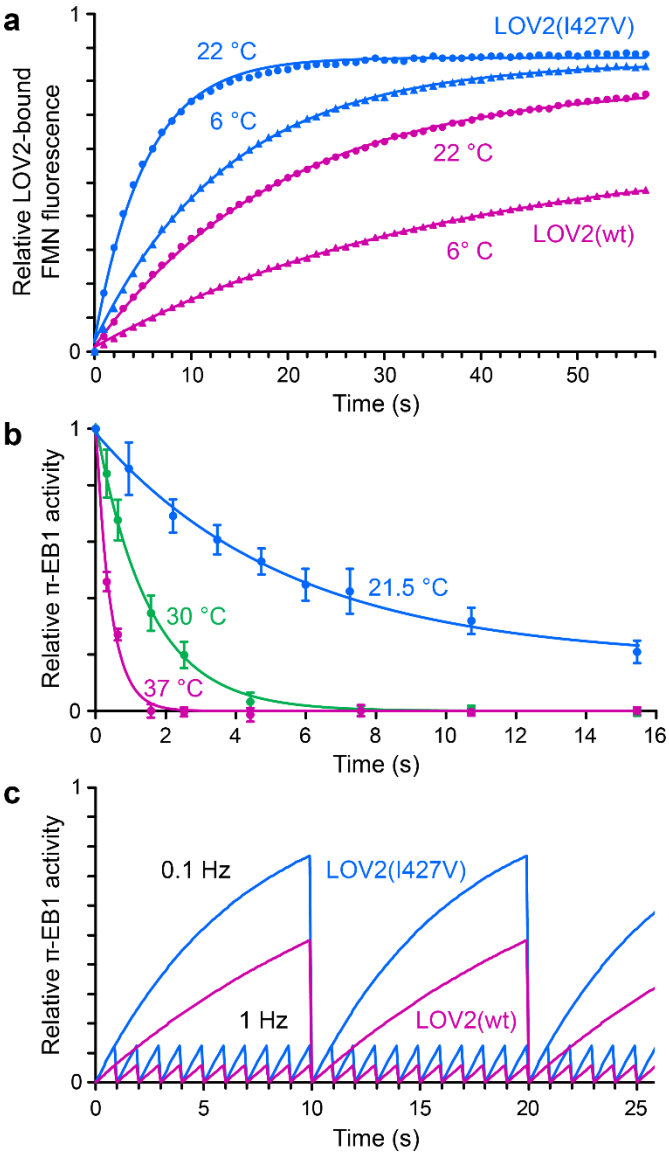

Fig. 3 Factors influencing π-EB1 photodissociation kinetics**.** (**a**) LOV2 reversion to the dark state is temperature sensitive and tunable. Dark state recovery was analyzed by measuring flavin fluorescence (λ_{Ex} = 475nm, λ_{Em} = 537/35 nm), which recovers upon flavin-cysteinyl adduct decay, at the indicated temperatures in *E. coli* colonies expressing a wild-type LOV2 domain or a fast cycling variant LOV2(I427V) after photoactivation with higher intensity 475 nm light. The LOV2 dark state recovery rate is a limiting factor in optogenetics experiments, because it impacts how much light is required to maintain a certain level of photoactivation. In addition, intracellular diffusion of photoactivated molecules limits spatial resolution. (**b**) Temperature sensitivity of π-EB1 photodissociation. π-EB1 activity was measured by monitoring the ratio of EGFP-Zdk1-EB1C on MT plus ends versus cytoplasm in time-lapse experiments at the indicated temperatures with identical blue light exposure

settings. π-EB1 photodissociation is much slower and inefficient at room temperature compared with 37 °C. (**c**) Comparison of the predicted π-EB1 activity levels at different saturating blue light pulse frequencies based on measured exponential recovery rates. For example, at a 1 Hz blue light pulse frequency wild-type LOV2 recovers to ~5% before the next blue light pulse hits. Because of the faster dark recovery, the fast cycling LOV2(I427V) variant would require an approximately two-fold higher blue light pulse frequency to maintain the same average activation state. 0.1 Hz is insufficient to maintain a high average π-EB1 photodissociation (>50% recovery before the next blue light exposure).

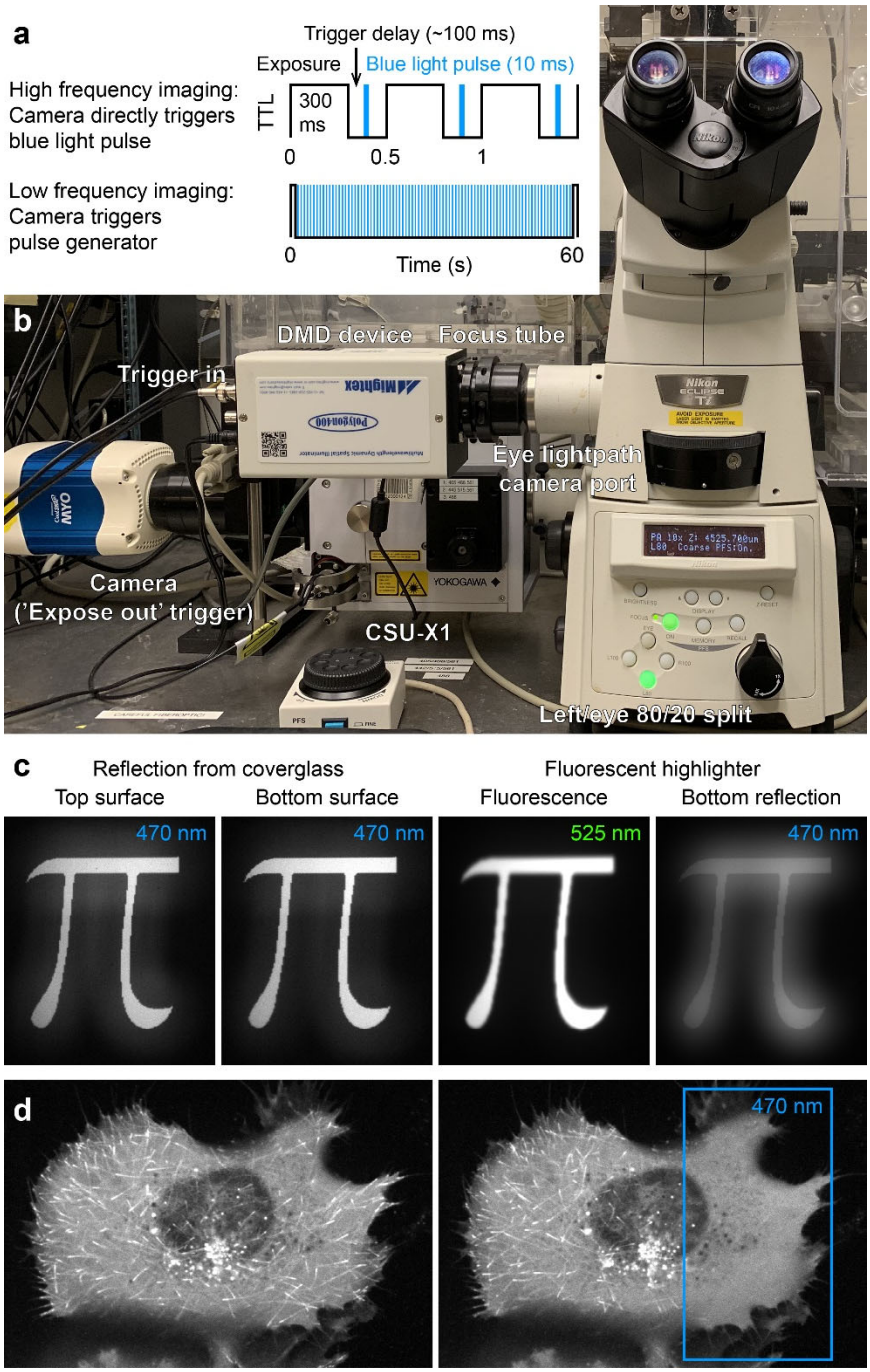

Fig. 4 Spatial control with a DMD device. (**a**) Schematic of the two methods triggering the DMD blue light pattern exposure depending on image acquisition rate. (**b**) Setup of the Polygon400 pattern illuminator on our spinning disk confocal microscope system through an additional camera port in the eyepiece lightpath. (**c**) Visualization of the blue light pattern. The left two panels show the reflection of the pattern (π symbol) on the top and bottom surface of a coverglass. Note the slight haze around the π symbol resulting from the out-of-focus reflection from

the other side of the coverglass. The two panels on the right show fluorescence of a yellow highlighter mark and the much less bright direct blue light reflection from the bottom coverglass surface. (**d**) Spatially restricted π-EB1 photodissociation. Cell expressing untagged EB1N-LOV2(I427V) and mCherry-Zdk1-EB1C. Images were acquired at 1 frame per second. 20 ms pulses of the DMD blue light pattern were triggered directly by the camera in between image acquisitions.

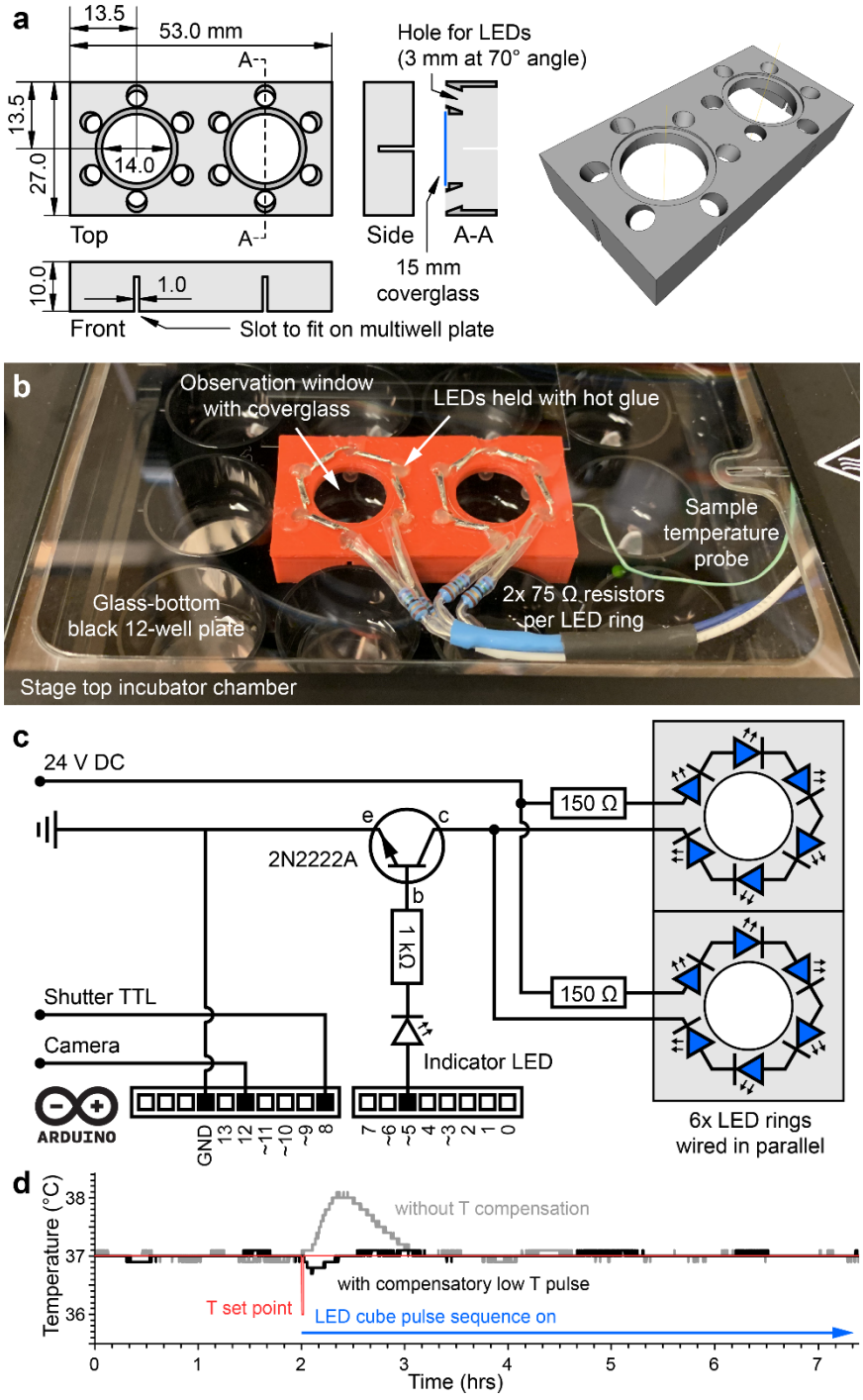

Fig. 5 DIY LED cube design for multiwell π-EB1 photodissociation. (**a**) Technical drawing of the 3D printed plastic part of the LED-cube (FreeCAD 3D file available upon request). (**b**) Image of the LED cube on a 12-well plate inside an Okolab stage top incubator. The LED power wires are threaded through holes in the side of the incubator chamber. Six LEDs are hot glued into the 3 mm holes and leads from adjacent LEDs are soldered together in series on top of the plastic part. (**c**) Circuit diagram of the Arduino-based LED pulse generator. (**d**)

Temperature trace inside a blue light exposed well before and after LEDs are turned on. A short low temperature pulse (1 min to 36 °C at the start of blue light exposure) effectively compensates for the transient temperature increase.

1. Losi A, Gardner KH, Möglich A (2018) Blue-Light Receptors for Optogenetics. Chem Rev 118:10659–10709. https://doi.org/10.1021/acs.chemrev.8b00163
2. Goglia AG, Toettcher JE (2019) A bright future: optogenetics to dissect the spatiotemporal control of cell behavior. Curr Opin Chem Biol 48:106–113. https://doi.org/10.1016/j.cbpa.2018.11.010
3. Huala E, Oeller PW, Liscum E, et al (1997) Arabidopsis NPH1: A protein kinase with a putative redox-sensing domain. Science 278:2120–2123. https://doi.org/10.1126/science.278.5346.2120
4. Christie JM, Salomon M, Nozue K, et al (1999) LOV (light, oxygen, or voltage) domains of the blue-light photoreceptor phototropin (nph1): Binding sites for the chromophore flavin mononucleotide. Proc Natl Acad Sci U S A 8779–8783. https://doi.org/10.1073/pnas.96.15.8779
5. Christie JM (2007) Phototropin Blue-Light Receptors. Annu Rev Plant Biol 58:21–45. https://doi.org/10.1146/annurev.arplant.58.032806.103951
6. Salomon M, Christie JM, Knieb E, et al (2000) Photochemical and mutational analysis of the FMN-binding domains of the plant blue light receptor, phototropin. Biochemistry 39:9401–9410
7. Harper SM, Neil LC, Gardner KH (2003) Structural basis of a phototropin light switch. Science 301:1541–1544. https://doi.org/10.1126/science.1086810
8. Konold PE, Mathes T, Weienborn J, et al (2016) Unfolding of the C-Terminal Jα Helix in the LOV2 Photoreceptor Domain Observed by Time-Resolved Vibrational Spectroscopy. J Phys Chem Lett 7:3472–3476. https://doi.org/10.1021/acs.jpclett.6b01484
9. Zayner JP, Antoniou C, Sosnick TR (2012) The amino-terminal helix modulates light-activated conformational changes in AsLOV2. J Mol Biol 419:61–74. https://doi.org/10.1016/j.jmb.2012.02.037
10. Kottke T, Xie A, Larsen DS, Hoff WD (2018) Photoreceptors Take Charge: Emerging Principles for Light Sensing. Annu Rev Biophys 47:291–313. https://doi.org/10.1146/annurev-biophys-070317-033047
11. Yao X, Rosen MK, Gardner KH (2008) Estimation of the available free energy in a LOV2-Jα photoswitch. Nat Chem Biol 4:491–497. https://doi.org/10.1038/nchembio.99
12. Wu YI, Frey D, Lungu OI, et al (2009) A genetically encoded photoactivatable Rac controls the motility of living cells. Nature 461:104–108. https://doi.org/10.1038/nature08241
13. Lungu OI, Hallett RA, Choi EJ, et al (2012) Designing Photoswitchable Peptides Using the AsLOV2 Domain. Chem Biol 19:507–517. https://doi.org/10.1016/j.chembiol.2012.02.006
14. Dagliyan O, Tarnawski M, Chu PH, et al (2016) Engineering extrinsic disorder to control protein activity in living cells. Science 354:1441–1444. https://doi.org/10.1126/science.aah3404
15. Reynolds KA, McLaughlin RN, Ranganathan R (2011) Hot spots for allosteric regulation on protein surfaces. Cell 147:1564–1575. https://doi.org/10.1016/j.cell.2011.10.049

16. Wang H, Vilela M, Winkler A, et al (2016) LOVTRAP: An optogenetic system for photoinduced protein dissociation. Nat Methods 13:755–758. https://doi.org/10.1038/nmeth.3926
17. Guntas G, Hallett RA, Zimmerman SP, et al (2015) Engineering an improved light-induced dimer (iLID) for controlling the localization and activity of signaling proteins. Proc Natl Acad Sci U S A 112:112–117. https://doi.org/10.1073/pnas.1417910112
18. Strickland D, Lin Y, Wagner E, et al (2012) TULIPs: Tunable, light-controlled interacting protein tags for cell biology. Nat Methods 9:379–384. https://doi.org/10.1038/nmeth.1904
19. Kumar P, Wittmann T (2012) +TIPs: SxIPping along microtubule ends. Trends Cell Biol. 22:418–428
20. van Haren J, Wittmann T (2019) Microtubule Plus End Dynamics − Do We Know How Microtubules Grow? BioEssays 41:e1800194. https://doi.org/10.1002/bies.201800194
21. van Haren J, Charafeddine RA, Ettinger A, et al (2018) Local control of intracellular microtubule dynamics by EB1 photodissociation. Nat Cell Biol 20:252–261. https://doi.org/10.1038/s41556-017-0028-5
22. Wittmann T, van Haren J (2018) Generation of cell lines with light-controlled microtubule dynamics. Protoc Exch. https://doi.org/10.1038/protex.2017.155
23. Grimm JB, Muthusamy AK, Liang Y, et al (2017) A general method to fine-tune fluorophores for live-cell and in vivo imaging. Nat Methods 14:987–994. https://doi.org/10.1038/nmeth.4403
24. Swartz TE, Corchnoy SB, Christie JM, et al (2001) The Photocycle of a Flavin-binding Domain of the Blue Light Photoreceptor Phototropin. J Biol Chem 276:36493–36500. https://doi.org/10.1074/jbc.M103114200
25. Kennis JTM, Crosson S, Gauden M, et al (2003) Primary reactions of the LOV2 domain of phototropin, a plant blue-light photoreceptor. Biochemistry 42:3385–3392. https://doi.org/10.1021/bi034022k
26. Eitoku T, Nakasone Y, Matsuoka D, et al (2005) Conformational dynamics of phototropin 2 LOV2 domain with the linker upon photoexcitation. J Am Chem Soc 13238–13244. https://doi.org/10.1021/ja052523i
27. Kottke T, Heberle J, Hehn D, et al (2003) Phot-LOV1: Photocycle of a blue-light receptor domain from the green alga Chlamydomonas reinhardtii. Biophys J 84:1192–1201. https://doi.org/10.1016/S0006-3495(03)74933-9
28. Laissue PP, Alghamdi RA, Tomancak P, et al (2017) Assessing phototoxicity in live fluorescence imaging. Nat Methods 14:657–661. https://doi.org/10.1038/nmeth.4344
29. Ettinger A, Wittmann T (2014) Fluorescence live cell imaging. Methods Cell Biol 123:77–94. https://doi.org/10.1016/B978-0-12-420138-5.00005-7
30. Zayner JP, Sosnick TR (2014) Factors that control the chemistry of the LOV domain photocycle. PLoS One 9:e87074. https://doi.org/10.1371/journal.pone.0087074

31. Kawano F, Aono Y, Suzuki H, Sato M (2013) Fluorescence imaging-based high-throughput screening of fast- and slow-cycling LOV proteins. PLoS One 8:e82693. https://doi.org/10.1371/journal.pone.0082693
32. Grzelak A, Rychlik B, Bartosz G (2001) Light-dependent generation of reactive oxygen species in cell culture media. Free Radic Biol Med 30:1418–1425. https://doi.org/10.1016/S0891-5849(01)00545-7
33. Zigler JS, Lepe-Zuniga JL, Vistica B, Gery I (1985) Analysis of the cytotoxic effects of light-exposed hepes-containing culture medium. Vitr Cell Dev Biol 21:282–287. https://doi.org/10.1007/BF02620943
34. Halliwell B, Butt VS (1972) Flavin mononucleotide-sensitized photo-oxidation of glyoxylate in Good's buffers. (Short Communications). Biochem J 129:1157–1158. https://doi.org/10.1042/bj1291157
35. Stockley JH, Evans K, Matthey M, et al (2017) Surpassing light-induced cell damage in vitro with novel cell culture media. Sci Rep 7:849. https://doi.org/10.1038/s41598-017-00829-x
36. Stehbens S, Pemble H, Murrow L, Wittmann T (2012) Imaging intracellular protein dynamics by spinning disk confocal microscopy. Methods Enzymol 504:293–313. https://doi.org/10.1016/B978-0-12-391857-4.00015-X
37. Christie JM, Corchnoy SB, Swartz TE, et al (2007) Steric interactions stabilize the signaling state of the LOV2 domain of phototropin 1. Biochemistry 46:9310–9319. https://doi.org/10.1021/bi700852w